

An Innovative Information Fusion Method with Adaptive Kalman Filtering for Integrated INS/GPS Navigation of Autonomous Vehicles

Yahui Liu, Xiaoqian Fan, Chen Lv, Jian Wu, Liang Li, Dawei Ding

State Key Laboratory of Automotive Safety and Energy, Tsinghua University, Beijing, 100083

Key words:

Integrated navigation
Information fusion
IAE-AKF
Autonomous vehicle

A B S T R A C T:

Information fusion method of INS/GPS navigation system based on filtering technology is a research focus at present. In order to improve the precision of navigation information, a navigation technology based on Adaptive Kalman Filter with attenuation factor is proposed to restrain noise in this paper. The algorithm continuously updates the measurement noise variance and processes noise variance of the system by collecting the estimated and measured values, and this method can suppress white noise. Because a measured value closer to the current time would more accurately reflect the characteristics of the noise, an attenuation factor is introduced to increase the weight of the current value, in order to deal with the noise variance caused by environment disturbance. To validate the effectiveness of the proposed algorithm, a series of road tests are carried out in urban environment. The GPS and IMU data of the experiments are collected and processed by dSPACE and MATLAB/Simulink. Based on the test results, the accuracy of the proposed algorithm is 20% higher than that of a traditional adaptive Kalman filter. It also shows that the precision of the integrated navigation can be improved due to the reduction of the influence of environment noise.

1 INTRODUCTION

In recent years, many research institutions and manufacturers in auto industry have invested heavily in the development of autonomous vehicles, in which navigation technology is of central concern. At present, the positioning accuracy of the navigation system is mainly ensured by using expensive sensors. For instance, in 2013 Sungisk Huh and David Hyunchul Shim used a laser navigation system for autonomous flight [1], but it would be too expensive for this system to be applied in mass-produced vehicles. Currently, autonomous vehicle is highly required of an integrated navigation system with low cost and high precision [2]. Laser radar would obtain accurate data, but the cost is too high. Methods based on information fusion and prediction algorithm can attain the same level of accuracy with affordable cost, offering much more promising solutions.

Integrated navigation is much advantageous over the single navigation system. Although the Global Position System (GPS) has a higher positioning accuracy than other positioning approaches, it is vulnerable to a wide-ranging variety of interferences, such as the multipath effect from radars, electromagnetic interference, block of signals and so on [3]. The inertial navigation system (INS) is a completely autonomous navigation system with good concealment, strong anti-interference ability, immunity to

meteorological conditions, etc [4,5]. Peter Stauffer used acceleration and angular rate from IMU to estimate the state of robots [6] and achieved good reliability. However, pure INS suffers from accumulated error. Thus, when the IMU is used alone, it results in greater error than other approaches.

In order to improve the accuracy of integrated navigation, the estimation algorithm based on integrated navigation has been widely investigated in recent years. Wei Wang and Zongyu Liu's work was focused on the combination of GPS and INS navigation research, using Kalman Filter and Extent Kalman Filter to compensate the error generated by information fusion [7]. Zhimin Chen and Yuanxin Qu used the algorithm of EKF in the study on GPS/INS Loose and tight coupling [8]. However, the adoption of KF or EKF is likely to result in divergence caused by modeling error, especially for those low quality inertial devices.

There are also other problems with Kalman Filtering [9], for example, filtering effect tends to degrade with filtering time as the estimation ratio increases with time. For nonlinear system, EKF is not an ideal estimation method. Therefore, some researches used UKF [10, 11] instead of the algorithms mentioned above. For a low-dynamic system, such as a typical automotive system, the effects

of EKF and UKF are almost the same, according to the theory provided by Toledo-Moreo [12], etc. LS-SVM was proposed in [13], where Xiyuan Chen and Yuan Xu used the algorithm of LS-SVM on the navigation for indoor mobile robots, and achieved good results. In the process of solution, the operation time and memory space would increase rapidly with the dimension of state matrix. Thus, this method is not suitable for vehicle navigation.

Abdel-Hafez provided the algorithm of ANFIS [14], but the huge amount of computation and long learning time generate a long delay of the system, which is not ideal for the real-time system of autonomous vehicles. Some researchers also used different combination forms of GPS and INS, Such as tightly-coupled GPS/INS navigation [15, 16], which is hard to be realized and too complex to be applied in most industrial products.

After three decades of low ebb, the research of Neural Network has gradually become a hot spot. In references [17, 18], both Jiancheng Fang and Velimir Cirovic utilized neural network to control three-axis gyro stabilized platform and longitudinal wheel slip, and the error of navigation decreased to different degrees. However, it is not a suitable candidate of fusion algorithm in the field of integrated navigation, because it is complicated to be realized and often takes a long time to train the parameters of neural network.

Although the methods mentioned above have achieved good results in some way, there are still some problems remaining unsolved. Because GPS noise composition is complicated, which includes not only white noise but also other random environment noise caused by surrounding buildings and electromagnetic disturbance, and INS model and noise uncertainties also lead to some difficulties for information fusion estimation.

Currently these issues are not well solved. Environment noise is part of GPS/INS noise, and it seriously affects the estimation accuracy. The problem is that GPS and INS noises are usually regarded synonymous with white noise with neglecting environment noise. In this way, estimation accuracy is seriously affected.

Thus, the algorithm proposed in this paper is named of Innovation Adaptive Estimation Adaptive Kalman Filtering (IAE-AKF) based on memory attenuation. IAE-AKF is a filter which is able to not only avoid filtering divergence but also eliminate the influence of environment noise. The proposed method obviously yields better results compared with other commonly used approaches of information fusion, including Kalman Filter and Neural network technology. In order to make full use of the newly observed information and effectively

suppress the GPS noise component from the surroundings, the attenuation memory factor is added to the observed sequence of innovation, reducing the impact of data collected in the past on filtering. To solve the problem that output noise of GPS includes not only white noise but also the influence caused by surrounding factors in urban environment, the method through increasing the weight of measurement value of the current time can be adopted. It is a good indicator of the output variation of the variance. In the process of filtering, the method takes advantage of the continuously modified value observed to rectify the uncertain parameter and suppress the noise of model.

The rest of this paper is organized as follows. Section 2 is the algorithm synthesis of the IAE-AKF based on memory attenuation. And in section 3 the model of GPS/INS is introduced and the mathematical Model is established. In Section 4 the experimental results and analysis of the results are presented. In the meantime, the comparison of the results of our method with those of other methods are also discussed. Finally, the conclusion is given.

2 INTEGRATED NAVIGATION ALGORITHM

2.1 Covariance matching based on innovation

In order to update the variance of the system and control the divergence of the model, it is necessary to judge whether the system is stable and choose a different way of emanative control. The updated observation value can provide a guidance to adjust the Kalman gain. When the Kalman filter works in a stable state, 95% value of the innovation sequence r_k will fall near zero mean within a range of 2σ , where σ is the theoretical variance explained in equation(1). Based on the above analysis, innovation sequence variance is adopted to measure the variation of the innovation value.

$$\sigma^2 = H_k P_{k,k-1} H_k^T + R_k \quad (1)$$

$$r_k = Z_k - H_k \hat{X}_{k,k-1} \quad (2)$$

$$\hat{C}_{r_k} = \frac{1}{N} \sum_{j=0}^k \mathbf{r}_j \mathbf{r}_j^T \quad (3)$$

where r_k is the innovation, \hat{C}_{r_k} is the estimation variance of the innovation sequence.

System model of Kalman Filtering is described as follows.

$$\begin{aligned} X_k &= \phi_{k,k-1} + \Gamma_{k-1} W_{k-1} \\ Z_k &= H_k X_k + V_k \end{aligned} \quad (4)$$

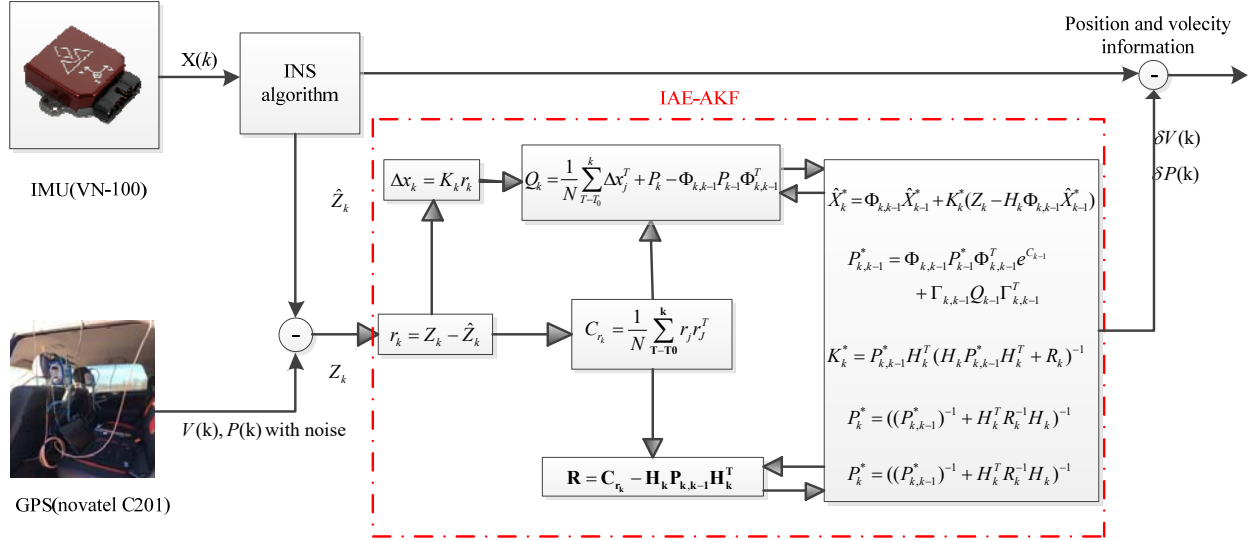


Fig.1. Process of IAE Kalman filtering

where $\phi_{k,k-1}$ is the transfer matrix of step; Γ_{k-1} is the matrix of noise driving; H_k is the measurement matrix; W_k is the noise excitation of the system; V_k is the measured noise. W_k and V_k are uncorrelated noises, meeting the demand that $E[W_k] = 0$, $\text{Cov}[W_k W_k] = Q_x$, $E[V_k] = 0$, $\text{Cov}[V_k V_k] = R_x$.

Rewrite the conventional formula of Kalman Filtering based on innovation adaptive form as follows according to reference [19].

State one-step predicting equation:

$$\hat{X}_{k+1} = \phi_{k,k-1} \hat{X}_k \quad (5)$$

State estimation equation:

$$\hat{X}_k = \hat{x}_{k,k-1} + K_r r_k \quad (6)$$

Kalman gain matrix:

$$K_k = P_{k,k-1} H_k^T C_{rk}^{-1} \quad (7)$$

$$C_{rk} = H_k P_{k,k-1} H_k^T + R_k \quad (8)$$

Error variance matrix of One-step predicting:

$$P_{k,k-1} = \phi_{k,k-1} P_{k-1} \phi_{k,k-1}^T + Q_k \quad (9)$$

Estimation error variance matrix:

$$P_k = (I - K_k H_k) P_{k,k-1} \quad (10)$$

Based on the zero mean white filter innovation sequence, the variance update equation of statistical noise matrix can be given by:

$$\hat{R}_k = \hat{C}_{rk} - H_k P_{k,k-1} H_k^T \quad (11)$$

$$\hat{Q}_k = \frac{1}{N} \sum_{j=0}^k \Delta x_j x_j^T + P_k + \Phi_{k,k-1} P_{k-1} \Phi_{k,k-1}^T \quad (12)$$

where $\Delta x_k = K_k r_k$. Combining equation (7) with equation (8), the modified K_k^* can be written as equation(13), where K_k is the IAE-AKF gain:

$$K_k^* = P_{k,k-1} H_k^T \left(\frac{1}{N} \sum_{j=0}^k r_j r_j^T \right) \quad (13)$$

The computation process is shown in Fig. 1

2.2 Attenuation Memory Filtering Algorithm

Since the interference of GPS is mainly caused by the surrounding buildings and other environment factors, it is not a fixed variance white noise. The introduction of attenuation factor can achieve a smaller value of the current signal deviation. And increasing the impact of new observational data is an effective way to overcome the filtering divergence. When the selected mathematical model is inaccurate, the most recent observations are more likely to be the accurate reflection of the actual situation than the previous ones. Thus, the memory attenuation factor is introduced so that the previous data can be ignored by the data.

In order to describe the algorithm clearly, the equation can be rewritten as:

$$\begin{aligned} X_k &= \phi_{k,k-1} X_{k-1} + \Gamma_{k-1} W_{k-1} \\ Z_k &= H_k X_k + V_k \end{aligned} \quad (14)$$

The basic idea of attenuation memory filter is to increase the weight of new observations. The method is to increase the value of Q_i , R_i , P_i in the filter formula. The process of Kalman filter is introduced in [20]. According to theory, the Kalman optimal gain matrix formula (15) can be obtained as [21]:

$$K_k = P_k H_k^T R_k^{-1} \quad (15)$$

From formula (15), it can be seen that K_k and R_k are inversely proportional to each other. In order to make better use of the observed information of the current time and reduce the weight of the old data. So the farther away from the current moment, the greater the value of R_k should be. Thus the method of exponential weighting is adopted in equation(16):

$$P_0^* = e^{\sum_{i=0}^{N-1} C_i} P_0, P_1^* = e^{\sum_{i=1}^{N-1} C_i} P_1, \dots \quad (16)$$

$$R_{N-1}^* = e^{C_{N-1}} R_{N-1}, R_N^* = R_N$$

where $C_i(i=1,2,\dots)$ is an appropriate integer. This form of weighting can attenuate the effect of previous value of measurements.

According to the Kalman filter formula , We can deduce the attenuation memory filter equations as follows.

$$\hat{X}_k^* = \Phi_{k,k-1} \hat{X}_{k-1}^* + K_k^* (Z_k - H_k \Phi_{k,k-1} \hat{X}_{k-1}^*) \quad (17)$$

$$K_k^* = P_{k,k-1}^* H_k^T (H_k P_{k,k-1}^* H_k^T + R_k)^{-1} \\ = P_k^* H_k^T R_k^{-1} \quad (18)$$

$$P_{k,k-1}^* = \Phi_{k,k-1} P_{k-1}^* \Phi_{k,k-1}^T e^{C_{k-1}} \\ + \Gamma_{k,k-1} Q_{k-1} \Gamma_{k,k-1}^T \quad (19)$$

$$P_k^* = (I - K_k^* H_k) P_{k,k-1}^* \\ = ((P_{k,k-1}^*)^{-1} + H_k^T R_k^{-1} H_k)^{-1} \quad (20)$$

where \hat{X}_k^* , K_k^* , $P_{k,k-1}^*$ and P_k^* substitute for the original \hat{X}_k , K_k , $P_{k,k-1}$ and P_k .

Compared with the traditional adaptive Kalman filter, the difference is that an attenuation factor was introduced to the formula (15), (16), (17) and (18).

Because $e^{C_{k-1}} > 1$, the equations can be rewritten as:

$$P_{k,k-1}^* > P_{k,k-1} \quad (21)$$

$$K_k^* > K_k$$

Thus, the weight of current date is strengthened.

Attenuation memory filter has many advantages, such as simplicity in computation, small computing load and flexible form.

In order to introduce the attenuation factor into the IAE-AKF, \hat{X}_k , K_k , $P_{k,k-1}$, P_k are replaced in the IAE-AKF with \hat{X}_k^* , K_k^* , $P_{k,k-1}^*$, P_k^* to realize the fusion of the algorithm.

3 DEVELOPMENT OF REFERENCE MODEL

In this section, we will establish the system model of INS and GPS. In the east-north-up navigation reference frame,

$$X(t) = [\Phi_E \ \Phi_N \ \Phi_U \ \delta V_E \ \delta V_N \ \delta V_U \ \delta L \ \delta \lambda \ \delta H \\ \varepsilon_x \ \varepsilon_y \ \varepsilon_z \ \Delta_x \ \Delta_y \ \Delta_z]$$

where $\mathbf{X}(t)$ is a system state vector with 15-dimension, Φ_E , Φ_N and Φ_U are vehicle's attitude rotation vector error from direction of east, north and up, respectively. δV_E , δV_N and δV_U are velocity errors; δL , $\delta \lambda$ and δH are position error of latitude, longitude and height, respectively. ε_x , ε_y and ε_z are gyro constant drifts, and Δ_x , Δ_y and Δ_z are accelerometer zero errors.

Firstly, we analyze and model the inertial navigation system error. For most gyroscopes, system error includes constant drift, first - order Markov processes and white noise, and satisfies:

$$\dot{\varepsilon}_i = \varepsilon_{bi} + \varepsilon_{ri} + \omega_{gi} \quad (22)$$

where ε_b , ε_r and ω_g represent the constant drift, first - order Markov processes, and white noise, respectively. i is the reference coordinate system with x , y and z axis. ε_{bi} only changes at the first time when gyro starts to work. Then ε_{ri} can be represented as:

$$\dot{\varepsilon}_{ri} = -\frac{1}{\tau_G} \varepsilon_{ri} + \omega_{ri} \quad (23)$$

Because ε_{ri} is the first-order Markov processes where τ_G is the time constant and ω_{ri} is the white noise with uncertain variance. In the design of the integrated navigation, because the gyro's slow drift component is small, meanwhile, in order to reduce the dimension of the integrated navigation Kalman filter, slow drift component is often ignored.

Accelerometer error consists of constant offset, correlation error and white noise. Because the value of the correlation error is small compared to that of other errors, it is ignored to simplify the model in this study. The error model is the same as the gyro model introduced above. So it can be given by equation (24).

$$\dot{\Delta}_{bi} = 0 \quad (24)$$

where $i=x, y, z$. Δ_{bi} is a constant offset, ω_{ai} is the white noise of the accelerometer.

For the INS, the correlation system is the east, north and up. Platform angular rate is

$$\omega_{cmd}^n = \begin{bmatrix} -\frac{V_E}{R_M + h} \\ \omega_{ie} \cos(L) + \frac{V_E}{R_N + h} \\ \omega \sin(L) + \frac{V_E \tan(L)}{R_N + h} \end{bmatrix} \quad (25)$$

where V_E , and V_N are the velocity from direction of east and north obtained by inertial navigation system,

respectively. R_N and R_M are the major axis and short axis of earth. Because of the error of INS, error also exists in ω_{cmd}^n . Defining ω_{ip}^p as the real platform angular rate, it can be represented as:

$$\omega_p^p = \omega_{cmd}^n + \delta\omega_{en}^n + \delta\omega_{ie}^n - \varepsilon_i^p \quad (26)$$

where ε_i^p is the error's projection of INS in navigation coordinate system. $\delta\omega_{ie}^n$ is the earth rotation error's projection and $\delta\omega_{en}^n$ is geographic coordinate error's projection which caused by the error of latitude and speed. Φ^n is the bias from platform coordinate system to real coordinate, and it satisfies the equation (27).

$$\hat{\Phi}^n = C_p^n \omega_{ip}^p - \omega_{cmd}^n \quad (27)$$

where Φ^n is $[\Phi_E, \Phi_N, \Phi_U]^T$ and C_p^n is the space transformation matrix from navigation coordinate to real coordinate.

Now, the space transformation matrix from vehicle correlation to navigation coordinate is defined as C_b^n . Therefore, the space transformation matrix from vehicle coordinate to real coordinate can be obtained. And the vehicle attitude rotation error [22] is illustrated as follows.

$$\begin{aligned} \hat{\Phi}^n &= C_p^n \omega_m^n + C_p^n \delta\omega_{ie}^p + C_p^n \delta\omega_{en}^p - C_p^n \varepsilon^p - \omega_m^n \\ &= C_p^n \omega_m^n + \delta\omega_{ie}^n + \omega_{en}^n - \varepsilon^n - \omega_m^n \end{aligned} \quad (28)$$

Then according to the differential equation of velocity.

$$\dot{V}_{en}^n = C_b^n f^b - (2\omega_{ie}^n + \omega_{en}^n) \times V_{en}^n + g^n \quad (29)$$

where V_{en}^n is the velocity from direction of east, north and up, but for the reason mentioned above, C_b^n has error, as well. Thus, the real value of C_b^n can be amended by \hat{C}_b^n , as shown in equation (30).

$$\hat{C}_b^n = (I - \Phi^n) C_b^n \quad (30)$$

where $\Phi^n = \begin{bmatrix} 0 & -\Phi_U & \Phi_N \\ \Phi_U & 0 & \Phi_E \\ -\Phi_N & \Phi_E & 0 \end{bmatrix}$

Meanwhile, ω_{ie}^n and ω_{en}^n also have errors. So real angular rate $\hat{\omega}_{ie}^n$ and $\hat{\omega}_{en}^n$ can be given by:

$$\hat{\omega}_{ie}^n = \omega_{ie}^n + \delta\omega_{ie}^n \quad (31)$$

$$\hat{\omega}_{en}^n = \omega_{en}^n + \delta\omega_{en}^n \quad (32)$$

Because of the error of acceleration, the real f^b is defined as:

$$\hat{f}^b = f^b + \Delta^b \quad (33)$$

The real value of V_{en}^n can be defined as \hat{V}_{en}^n , as equation (34) shows in the following.

$$\dot{\hat{V}}_{en}^n = \hat{C}_b^n \hat{f}^b - (2\hat{\omega}_{ie}^n + \hat{\omega}_{en}^n) \times \hat{V}_{en}^n + g^n \quad (34)$$

According to equation (29) and (34),

$$\delta\dot{V}_{en}^n = \dot{\hat{V}}_{en}^n - \dot{V}_{en}^n \quad (35)$$

Substituting equation (28), (29), (30), (31) (32) and (33) into equation (35), the dynamics of V_{en}^n can be obtained as:

$$\begin{aligned} \delta\dot{V}_{en}^n &= -\Phi^n f^n + C_b^n \Delta^b - (2\omega_{ie}^n + \delta\omega_{ie}^n) \\ &\quad \times V_{en}^n - (2\delta\omega_{ie}^n + \delta\omega_{en}^n) \times V_{en}^n \\ &\quad - (2\omega_{ie}^n + \omega_{en}^n) \times V_{en}^n + g^n \end{aligned} \quad (36)$$

After obtaining the error of velocity, the position error can be figured out. Then states of position error can be established as:

$$\delta\dot{L} = \delta V_N \frac{1}{R_M + h} - \delta h \frac{V_N}{(R_M + h)^2} \quad (37)$$

$$\begin{aligned} \delta\dot{\lambda} &= \delta V_E \frac{secL}{R_N + h} + \delta L \frac{V_E tanL secL}{R_N + h} \\ &\quad - \delta h \frac{V_E secL}{(R_N + h)^2} \end{aligned} \quad (38)$$

$$\delta\dot{h} = \delta V_U \quad (39)$$

From the above description, we can obtain the state of GPS/IMU. The system state transition matrix $A(t)$ can be written as follows:

$$A(t) = \begin{bmatrix} F_{3 \times 3} & F_{3 \times 3}^* & E_{3 \times 3} & T_{3 \times 6} \\ F_{3 \times 3}^* & F_{3 \times 3}^{**} & E_{3 \times 3}^* & T_{3 \times 6}^* \\ 0_{3 \times 3} & F_{3 \times 3}^{**} & E_{3 \times 3}^* & 0_{3 \times 3} \\ 0_{6 \times 3} & 0_{6 \times 3} & 0_{6 \times 3} & E_{6 \times 6}^{**} \end{bmatrix}$$

The matrix $B(t)$ can be given by:

$$B(t) = \begin{bmatrix} C_b^n & 0_{3 \times 3} \\ 0_{3 \times 3} & C_b^n \\ 0_{9 \times 3} & 0_{9 \times 3} \end{bmatrix}$$

where $F_{3 \times 3}^*$, $F_{3 \times 3}^{**}$, $F_{3 \times 3}^*$, $F_{3 \times 3}^{**}$, $F_{3 \times 3}^*$, $F_{3 \times 3}^{**}$, $E_{3 \times 3}$, $E_{3 \times 3}^*$, $E_{3 \times 3}^*$, $E_{3 \times 3}^{**}$, $E_{6 \times 6}^{**}$, $T_{3 \times 6}$, $T_{3 \times 6}^*$ can be represented individually as:

$$F_{3 \times 3} = \begin{bmatrix} 0 & \omega_{ie} \sin L + \frac{V_E \tan L}{R_N + h} & (\omega_{ie} \cos L + \frac{V_E}{R_N + h}) \\ -(\omega_{ie} \sin L + \frac{V_E \tan L}{R_N + h}) & 0 & -\frac{V_N}{R_M + h} \\ \omega_{ie} \cos L + \frac{V_E}{R_N + h} & \frac{V_N}{R_M + h} & 0 \end{bmatrix}$$

$$F_{3 \times 3}^* = \begin{bmatrix} 0 & -f_u & f_n \\ f_u & 0 & f_e \\ -f_n & f_e & 0 \end{bmatrix}$$

$$F_{3 \times 3}^* = \begin{bmatrix} 0 & -\frac{1}{R_M + h} & 0 \\ \frac{1}{R_N + h} & 0 & 0 \\ \frac{\tan L}{R_N + h} & 0 & 0 \end{bmatrix}$$

$$F_{3 \times 3}^m = \begin{bmatrix} 0 & \frac{1}{R_M + h} & 0 \\ \frac{\sec L}{R_N + h} & 0 & 0 \\ 0 & 0 & 1 \end{bmatrix}$$

$$E_{3 \times 3} = \begin{bmatrix} 0 & 0 & 0 \\ -\omega_{ie} \sin L & 0 & 0 \\ \omega_{ie} \cos L + \frac{V_E}{R_N + h} \sec^2 L & 0 & 0 \end{bmatrix}$$

$$F_{3 \times 3}^* = \begin{bmatrix} \frac{V_N \tan L}{R_N + h} - \frac{V_U}{R_N + h} & 2\omega_{ie} \sin L + \frac{V_E \tan L}{R_N + h} & \left(2\omega_{ie} \cos L + \frac{V_E}{R_N + h} \right) \\ -2\omega_{ie} \sin L + \frac{V_E \tan L}{R_N + h} & -\frac{V_U}{R_M + h} & -\frac{V_N}{R_M + h} \\ 2\left(\omega_{ie} \cos L + \frac{V_E}{R_N + h} \right) & \frac{2V_N}{R_M + h} & 0 \end{bmatrix}$$

$$E_{3 \times 3}^* = \begin{bmatrix} 0 & 0 & 0 \\ \frac{V_E \sec L \tan L}{R_N + h} & 0 & 0 \\ 0 & 0 & 0 \end{bmatrix}$$

$$E_{3 \times 3}^i = \begin{bmatrix} 2\omega_{ie} \cos L V_N + \frac{V_E V_N}{R_N + h} \sec^2 L + 2\omega_{ie} \sin L V_U & 0 & 0 \\ -(2\omega_{ie} \cos L V_E + \frac{V_E^2}{R_N + h} \sec^2 L) & 0 & 0 \\ -2\omega_{ie} \sin L V_E & 0 & 0 \end{bmatrix}$$

$$E_{3 \times 3}^n = \text{diag}[-\alpha, -\alpha, -\alpha, -\beta, -\beta, -\beta]$$

$$T_{6 \times 6} = \begin{bmatrix} C_b^n & 0_{3 \times 3} \end{bmatrix}$$

$$T_{6 \times 6}^i = \begin{bmatrix} 0_{3 \times 3} & C_b^n \end{bmatrix}$$

The integrated navigation usually uses the position difference given by GPS receiver and IMU system, and the velocity output difference given by them as the measured values. We define velocity of the east and north from IMU as V_{ie} , V_{in} , respectively, and define longitude and latitude from IMU as λ_i , L_i , and define V_{ge} , V_{gn} as the velocity of east and north from GPS. λ_g and L_g represent the position information from GPS. Then we can :

$$V_{ie} = V_e + \delta V_{ie} \quad (40)$$

$$V_{in} = V_n + \delta V_{in} \quad (41)$$

$$V_{ge} = V_e + \delta V_{ge} \quad (42)$$

$$V_{gn} = V_n + \delta V_{gn} \quad (43)$$

where λ , L is the real position.

$$\lambda_i = \lambda + \delta \lambda_i \quad (44)$$

$$L_i = L + \delta L_i \quad (45)$$

$$\lambda_g = \lambda + \delta \lambda_g \quad (46)$$

$$L_g = L + \delta L_g \quad (47)$$

where λ , L is the real position.

The observation equation is written as follows:

$$Z = H(t)X(t) + \omega(t) \quad (48)$$

where $\omega(t)$ is the measurement noise.

The error of measurement can be defined as:

$$Z = \begin{bmatrix} V_{ie} - V_{ge} \\ V_{in} - V_{gn} \\ \lambda_i - \lambda_g \\ L_i - L_g \end{bmatrix} \quad (49)$$

$$H(t) = \begin{bmatrix} 0 & 0 & 0 & 1 & 0 & 0 & 0 & 0 & 0 & \dots \\ 0 & 0 & 0 & 0 & 1 & 0 & 0 & 0 & 0 & \dots \\ 0 & 0 & 0 & 0 & 0 & 0 & 1 & 0 & 0 & \dots \\ 0 & 0 & 0 & 0 & 0 & 0 & 0 & 1 & 0 & \dots \end{bmatrix}_{4 \times 15} \quad (50)$$

4 EXPERIMENT RESULT

This experiment uses the MEMS device (VN-100 Rugged IMU). The IMU's performance is quite satisfactory because that accelerometer and gyroscope are installed within the same QFN package, minimizing cross coupling errors and relaxing the calibration requirements.

Table 1. IMU parameters

IMU parameter	Parameter Value
INS out frequency	100HZ
Gyro range	$\pm 2000^\circ / s$
Gyro bias	$\pm 0.05^\circ / s$
Accelerometer range	$\pm 16g$
Accelerometer bias	0.4mg

A low-cost GPS, the Novatel C201, is connected to the RPi-2. In order to reduce the system's cost, the single antenna GPS is chosen. The GPS antenna is mounted on the top of the vehicle. This GPS is ideal for our testing because it provides a variety of navigation solution with

position, velocity, and standard deviations. Our estimated results can be verified in the difference mode of GPS.



Fig.2. Instrument of this experiment

In our study, urban roads around Beijing is chosen as the test routes. The Auto-box is adopted as the communication device between MATLAB and IMU/GPS, and processes the date using MATLAB/Simulink.

Fig. 3 and Fig. 4 show the data of acceleration and angular rate obtained from IMU. A_x , A_y and A_z are the longitudinal acceleration, lateral acceleration and vertical acceleration of vehicle for vehicle coordinate system, respectively. It consists of real value, white noise and zero offset. As shown in Fig 8, if these data is not filtered, the result would be with large errors.

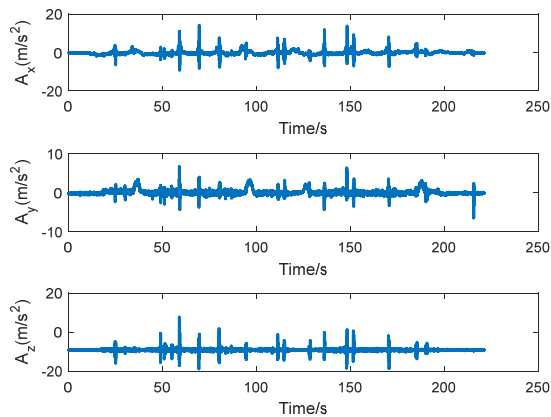


Fig.3. Acceleration of IMU with noise

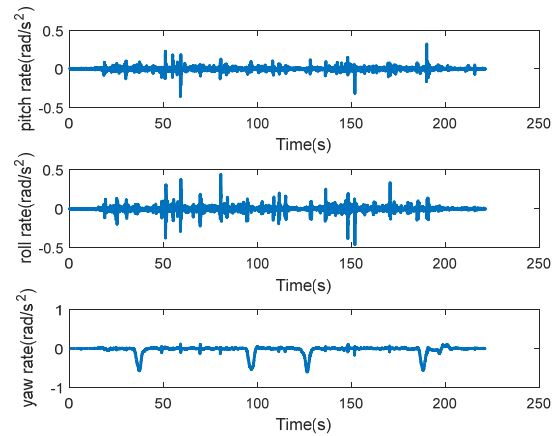


Fig.4. Angular rate of IMU with noise

Fig.5 illustrates the date of single antenna GPS and IMU. The track obtained from GPS shows that because of the environment influence and some other disturbances, the track fluctuates randomly. If we continue to regard these fluctuations as white noise, there would be of a big error. Hence, it is important to introduce weighting factor. The IMU can overcome the fluctuation effectively. Fig. 5 also shows that though the track obtained from IMU is smooth, the accuracy is lower than that of GPS because of white noise.

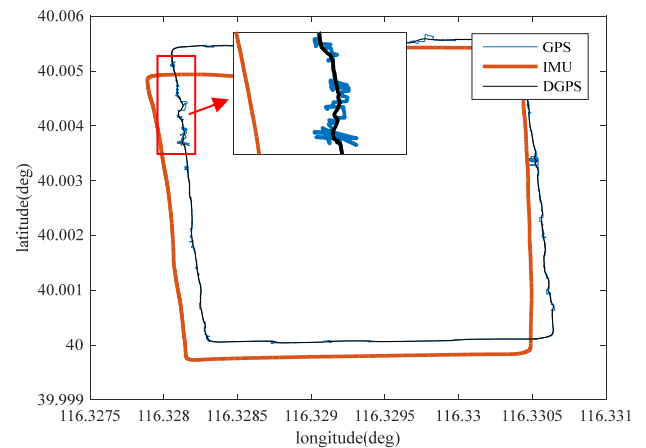


Fig.5. Different track of vehicle

Fig. 6 shows the performance of conventional adaptive Kalman Filter, IAE-AKF and single GPS. As shown in this figure, in some cases the effect of GPS is more accurate than that of other methods, but when it is affected by environmental factors the error changes violently, that is unfavorable for real-time control of the vehicle. Fig.6 also illustrates that the effect of IAE-AKF is significantly better than conventional Kalman Filtering. The experiment result shows that the performance of the IAE-AKF is also better than that of GPS, because the curve is smoother than that given by GPS.

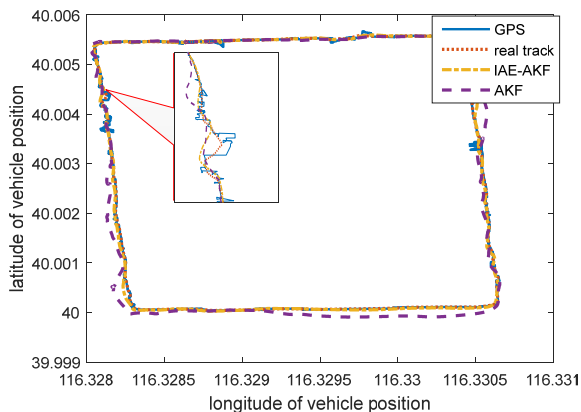


Fig.6. Comparison of track between different algorithm

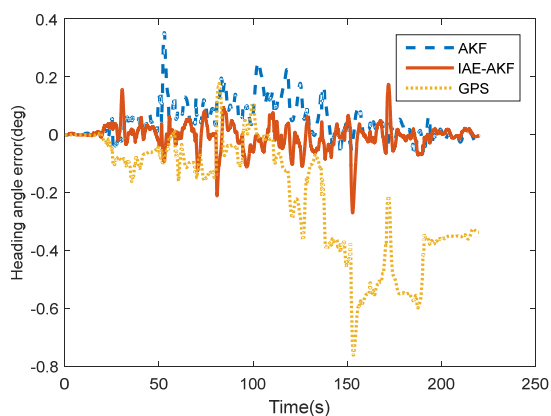


Fig.7. Comparison of heading angle error between different algorithm

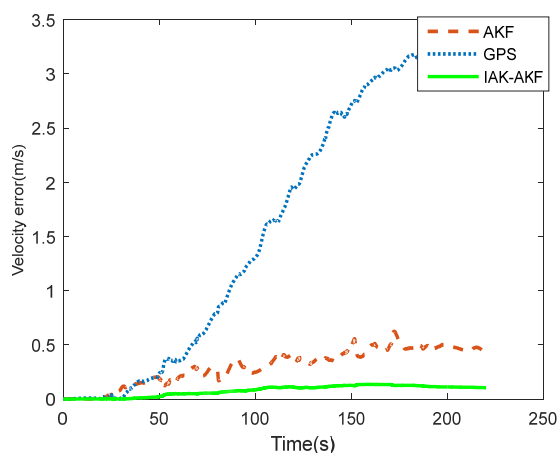


Fig.8. Comparison of Velocity error between different algorithm

A method is presented for GPS/INS integrated navigation system based on attenuation factor in this paper. And the validity and superiority of the algorithm are verified by experiments. As shown in Fig. 7, Fig.8 and Fig.9, IAE-AKF filter provides better accuracy in heading

angle, velocity and anti-interference capability. Because of the introduction of Attenuation coefficient, the Kalman gain K can be adjusted more effectively.

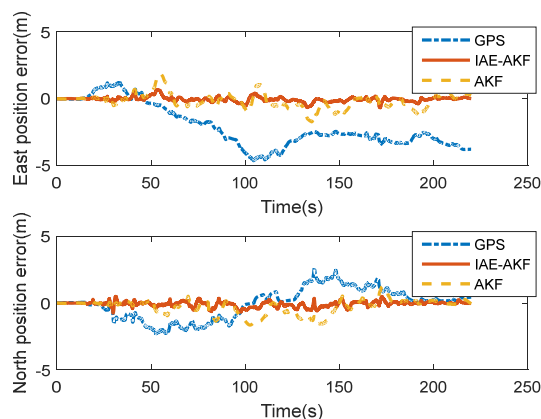


Fig.9. Error of distance between different algorithm

5 CONCLUSION

For a complicated integrated GPS/IMU system with an uncertain dynamic model, the traditional filtering method is no longer applicable. In this paper, a new filtering algorithm is proposed for inaccurate integrated system. And the parameter uncertainty of noise are described by innovation. The introduction of attenuation factor avoids the divergence of Kalman Filtering and improves the utilization rate of observation data of the filter. The IAE-AKF based on attenuation factor algorithm reconstructs the structure of Kalman Filtering. And the validity and superiority of the algorithm are verified by experiments. In the same conditions, AKF exhibits larger fluctuations. When environment noise changes, IAE-AKF can better amplify the value of the filter variance R , and gain K is automatically reduced, decreasing the influence of noise on the result, validating the feasibility and effectiveness of the proposed algorithm.

REFERENCE

- [1] Sungisk Huh, David Hyunchul Shim. Integrated Navigation System using Camera and Gimbaled Laser Scanner for Indoor and Outdoor Autonomous Flight of UAVs. IEEE Intelligent Robots and Systems 2013; DOI: 10. 1109/IROS. 6696805.
- [2] Setareh Yazdkhasti, Jurek Z.Sasiadek. Performance Enhancement for GPS/INS Fusion by Using a Fuzzy Adaptive Unscented Kalman Filter. IEEE Conference Publications 2016. 10: 1194 – 1199.
- [3] Isaac Skog, In-Car Positioning and Navigation Technologies - A Survey. IEEE trans on Intelligent Transportation 2009. 10: NO.1.
- [4] H.Poor. Performance Enhancement of MEMS-Based INS/GPS Integration for Low-Cost

- Navigation Applications, IEEE trans on Vehicular Technology 2009. 58: NO.3.
- [5] Zhao Rui, Gu Qitai. Optimal nonlinear filter for INS alignment. Tsinghua Science And Technology 2002. ISSN 1007-0214 10/22:263 – 269. 7: NO.3.
- [6] Peter Staufer, Hubert Gatttringer. State estimation on flexible robots using accelerometers and angular rate sensors. Mechatronics 2012; 22:1043-1049.
- [7] Wei Wang, Zongyu Liu. Quadratic extended Kalman filter approach for GPS/INS integration. Aerospace Science and Technology 2006, 10:709-719.
- [8] Zhimin Chen, Yuanxin Qu, Xiaodong Ling. Study on GPS/INS Loose and Tight Coupling. Intelligent Human-Machine Systems and Cybernetics 2015.
- [9] Hyungjik Lee, Seul Jung. Balancing and navigation control of a mobile inverted pendulum robot using sensor fusion of low cost sensors. Mechatronics 2012; 22:95-105.
- [10] Gaoge Hu; Shesheng Gao, A derivative UKF for tightly coupled INS/GPS integrated navigation. ISA Trans 2015. 56: 135–144.
- [11] Rhudy M, Gu Y, Gross J, et al. Evaluation of matrix square root operations for UKF within a UAV GPS/INS sensor fusion application. International Journal of Navigation and Observation 2011.
- [12] Adam Werries. Adaptive Kalman Filtering Methods for Low-Cost GPS/INS Localization for Autonomous Vehicles. Robotics Commons 2016.
- [13] Xiyuan Chen, Yuan Xu. Improving ultrasonic-based seamless navigation for indoor mobile robots utilizing EKF and LS-SVM. Measurement 2016. 92: 243-251
- [14] Mohammad Abdel Kareem Jaradat, Mamoun F. Abdel-Hafez. Enhanced, Delay Dependent Intelligent Fusion for INS/GPS Navigation System. IEEE SENSORS JOURNAL 2014. DOI: 10.1109/JSEN.2014.2298896.
- [15] Y. Zhao, M. Becker. Improving the performance of tightly-coupled GPS/INS navigation by using time-differenced GPS-carrier-phase measurements and low-cost MEMS IMU. Gyroscopy and Navigation 2015. 6: 133–142.
- [16] J. WENDEL, J. METZGER. A Performance Comparison of Tightly Coupled GPS/INS Navigation Systems based on Extended and Sigma Point Kalman Filters. The Institute of Navigation 2006. 53: 21–31.
- [17] Jiancheng Fang, Rui Yin. An adaptive decoupling control for three-axis gyro stabilized platform based on neural networks. Mechatronics 2015. 27: 38–46.
- [18] Velimir Cirovic, Dragan Alekesendric. Longitudinal wheel slip control using dynamic neural networks Original Research Article. Mechatronics 2013. 23: 135-146.
- [19] Hoda Sadeghian; Hassan Salarieh. On the general Kalman filter for discrete time stochastic fractional systems Original Research Article. Mechatronics 2013. 23: 764-771.
- [20] Kai Pan, Mingrong Ren. A federated filtering personal navigation algorithm based on MEMS-INS/GPS integrated. Chinese Control and Decision Conference 2016.
- [21] Alberto Cavallo, Giuseppe De Maria, Ciro Natale, Salvatore Pirozzi. Slipping detection and avoidance based on Kalman filter. Mechatronics 2014. 24: 489-499.
- [22] Kui Li, Jiaying Zhao. Federated ultra-tightly coupled GPS/INS integrated navigation system based on vector tracking for severe jamming environment. IET Radar, Sonar and Navigation 2015. 10: 1030 – 1037.